

FABRICATION STUDIES OF A 650 MHz SUPERCONDUCTING RF DEFLECTING MODE CAVITY FOR THE ARIEL ELECTRON LINAC

Douglas W. Storey^{†,1,2}, Robert E. Laxdal², Ben Matheson², Norman Muller²
¹University of Victoria, Victoria, Canada, ²TRIUMF, Vancouver, Canada

Abstract

A 650 MHz RF deflecting mode cavity is required for the ARIEL electron Linac to separate interleaved beams bound for either rare isotope production or a recirculation loop containing a Free Electron Laser. An RF separator will allow both modes to run simultaneously by imparting opposite transverse deflection to adjacent bunches at 1.3 GHz. The SRF cavity has been designed to provide up to 0.6 MV transverse voltage for operation with up to a 50 MeV CW electron beam. The design was optimised for compact geometry with high shunt impedance. Due to the low dissipated power, the cavity will operate at 4 K and allows for investigations into low cost fabrication techniques. The cavity is being machined from bulk reactor grade ingot Niobium and welds will be performed using TIG welding in an ultra-pure Argon chamber. Results of fabrication studies will be presented as well as measurements performed on a copper prototype cavity.

INTRODUCTION

The ARIEL electron linac (e-Linac) will deliver a 10 mA CW electron beam at an energy of 30 MeV to TRIUMF's new ARIEL facility to drive the production of rare isotopes [1]. A planned extension of the e-Linac would add a recirculation loop, allowing for a portion of the beam to be operated as an Energy Recovery Linac (ERL) while driving a free electron laser in the back leg of the loop. Simultaneous delivery of beam to both rare isotope production and the ERL is possible by interleaving the beams, requiring RF separation after the accelerator cavities to separate adjacent bunches.

A 650 MHz RF separator cavity will provide opposing transverse deflection to bunches occupying adjacent RF buckets of the 1.3 GHz accelerating RF. The required deflecting voltage is nominally 0.3 MV to initiate the separation of the two beams, which will be further separated by a quadrupole magnet and septum within a 3 meter distance. Deflecting voltages of up to 0.6 MV are considered to provide flexibility of the final design.

DESIGN

The geometry of the separator cavity (Figure 1) was modified from the RF Dipole cavity geometry that was developed for the Hi-Lumi LHC upgrade [2]. The cavity operates in a TE-like mode, with the transverse electric field between the ridges forming the main contribution to the deflecting field. The shape of the ridge was modified from the RF Dipole geometry to increase the shunt impedance by reducing the contribution to the deflecting

field from the magnetic field. This was achieved by modifying the ridge shape to pull the magnetic field away from the cavity axis. This increase in shunt impedance results in increased peak electric and magnetic fields on the ridges, although these remain low for the required deflecting voltages. Another goal of the modifications was to make the cavity shorter to decrease its longitudinal footprint in the beamline, resulting in a cavity geometry with ~50% higher shunt impedance and about half the relative length than other non-TM SRF deflecting cavity designs.

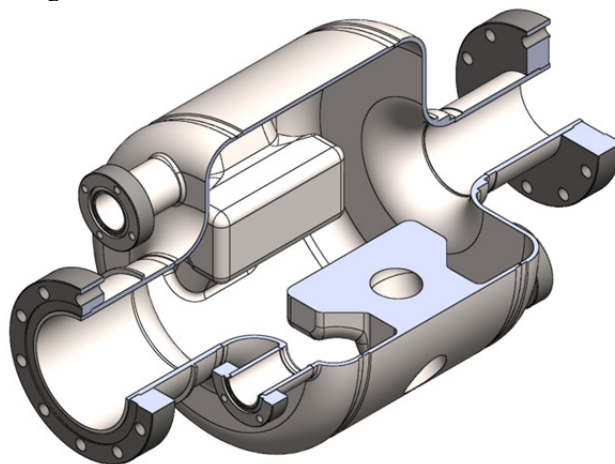


Figure 1: The cavity geometry showing the modified ridge shape. The “undercuts” allow the magnetic field to circulate around the ridges, decreasing the on axis magnetic field component.

The resulting cavity design provides the required deflecting voltage within a compact cavity with high shunt impedance and low RF power dissipation. The cavity will operate at 4.2 K, simplifying the cryomodule design and making use of the helium services supplying the e-Linac accelerating cavities.

The cavity has three small diameter RF ports on the ends of the cavity that will be used for the input coupler, higher order mode (HOM) coupler, and pickup probe. These ports will also be used to provide access for high pressure water rinsing of the cavity to provide coverage of the entire RF surface. The beam pipe on the upstream side of the cavity has a larger diameter to contain a resistive, coaxial HOM damper.

The full cavity design has been presented in [3], and a summary of the RF performance parameters are listed in Table 1.

[†] dstorey@triumf.ca

Table 1: Cavity Performance Parameters

Parameter	Value	Unit
Resonant frequency	650	MHz
Inner Diameter	204	mm
Inner Length	175	mm
Aperture	50	mm
Deflecting voltage	0.3 – 0.6	MV
Shunt impedance, R_{\perp}/Q	625	Ω
Geometry Factor	99	Ω
Peak electric field	9.5 – 19	MV/m
Peak magnetic field	12 – 24	mT
RF power dissipation at 4.2 K	0.35 – 1.4	W

FABRICATION TECHNIQUES

Due to the modest required deflecting voltage, the cavity will be fabricated using non-standard fabrication methods. In order to stabilize the cavity against pressure fluctuations to the goal of less than 10 Hz/mbar, the ridges will be machined from solid niobium. This is additionally advantageous since the shape of the ridges would be difficult to fabricate using standard methods. The remaining cavity walls will have a thickness of 3 mm, resulting in a simulated pressure sensitivity of the supported cavity of about 1 Hz/mbar.

To offset the cost of the large quantity of niobium required to fabricate solid ridges, bulk reactor grade niobium will be used to fabricate all parts. Three 214 mm diameter cylinders of niobium were purchased from Ningxia, with a measured RRR of 45. These will be used to machine the centre body and end caps, with the beam pipes and RF ports machined from the offcuts from the body piece. Figure 2 shows an exploded view of the cavity components.

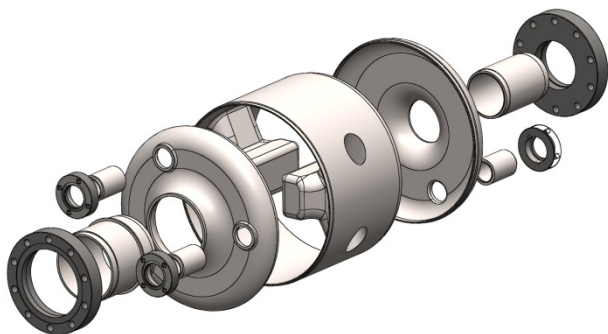


Figure 2: An exploded view of the cavity.

RF simulations with thermal feedback have been performed using ANSYS, showing no significant temperature rise of the RF surfaces, and good stability to normal conducting defects up to 100 μm diameter at 0.6 MV deflecting voltage. Cooling channels machined into the ridges will increase the cooling efficiency by allowing the liquid helium closer to the ridge faces.

The rough shape of the cavity has been cut by wire Electric Discharge Machining (EDM) to save the offcut material for future use. At least 1 mm of material will be

machined from all surfaces to remove any possible contamination, although it has previously been shown that a light chemical etch is generally sufficient for EDM surfaces [4]. The final surfaces will be machined by a CNC mill.

The welds on the cavity are all located in low field regions, with the peak magnetic field on the welds of only 8 mT at the maximum required deflecting voltage. Due to the low risk location of the cavity welds, welding will be performed by TIG welding inside of a glove box purged with argon. A procedure has been developed at TRIUMF, building upon previous coupon studies performed at MSU [5].

Weld studies were performed by welding together 2 mm thick by 12 mm wide coupons of both high RRR grade and reactor grade niobium. Etched weld coupons were inserted into a glove box and purged with ultra-high purity (grade 5.0) argon measured to contain less than 0.5 parts per million (ppm) oxygen. The oxygen concentration in the glove box was continuously monitored during welding by a GE O2X1 oxygen transmitter sensor.

The coupons were welded under varying oxygen concentrations to determine the reduction in the niobium's purity due to the diffusion of contaminants from the surrounding gas into the hot niobium during a weld. Argon was purged directly onto either side of the weld during the welding for 4 minutes after each weld was completed. Once completely cooled, the welded samples were removed from the glove box.

The RRR of the welded material was measured after welding, and compared to the RRR of the material the coupons were cut from. These measurements were performed on 5 mm wide strips machined from the welded region of the samples using a 4-wire resistance measurement at room temperature and at ~ 9.5 K, just before the superconducting transition, by cooling the samples in a helium gas flow cryostat. The RRR values reported here are defined by:

$$RRR = \frac{R_{300K}}{R_{9.5K}} = \frac{V_{300K}}{V_{9.5K}} \quad (1)$$

The results of all of the welds performed over several months of testing are shown in Figure 3. With an oxygen concentration of less than 10 ppm in the glove box, the reduction in RRR of the RRR grade Nb was limited to 20-25%. The degradation for reactor grade Nb was even less, with the RRR dropping by only $\sim 10\%$, from 45 to 40 post-weld. A clear trend exists, and it is expected that decreasing the oxygen concentration further would lead to negligible degradation of RRR.

If the material was welded twice, as it would be at the end of a circumferential weld or if a weld had to be repeated, the RRR was found to decrease more than for a single pass. For RRR niobium welded with ~ 7 ppm oxygen, the decrease in RRR was measured to be $\sim 25\%$ for one weld and $\sim 50\%$ for two overlapping welds.

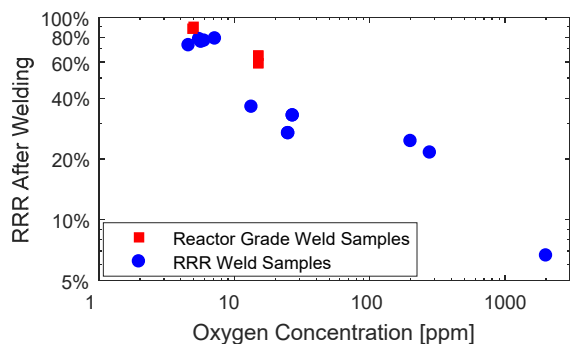


Figure 3: The relative RRR measured after TIG welds performed in the glove box with different ambient oxygen concentrations, compared to the pre-weld RRR.

The cavity welds will be performed in the glove box with less than 10 ppm oxygen and purging both upper and lower surfaces with argon. As the welds are all circumferential welds on circular components, the TIG welding will be semi-automated with the clamped cavity components mounted to a rotating fixture and the TIG torch fixed on a stand to achieve a consistent weld.

The beam pipe and RF port flanges are Grade 5 Titanium and will be welded to the niobium tubes using a small electron beam welder. A titanium jacket has been designed that will be welded to the beam pipes and the RF port flanges.

PROTOTYPE STUDIES

A copper prototype cavity was fabricated (Figure 4) to test the fabrication procedures and to allow low power field measurements of the cavity. The cavity was machined from solid copper in the same fashion as the niobium cavity using EDM and CNC milling, but was brazed instead of welded.



Figure 4: The copper prototype cavity

The centre body piece was intentionally made 15 mm long to test the tuning procedure required to reach the goal room temperature frequency. The two ends of the centre piece were trimmed based on frequency measurements made from the RF stack-up and comparing to RF simulation results. Following a 2-step trimming, the resonant frequency of the completed prototype cavity was 648.96, requiring only a small longitudinal plastic deformation to reach the goal frequency of 649.06 MHz.

The pressure sensitivity simulations were confirmed by pumping the cavity to vacuum and measuring a resulting

change in resonant frequency of 390 kHz. This compares to the simulated frequency shift for an unsupported copper cavity of 330 kHz.

Bead pull measurements of the operating mode and higher order modes (HOMs) were performed to determine their on axis electric field profile. These measurements show good agreement to the field profile simulated using HFSS for all of the modes measured up to 3 GHz. The measured field profile of the operating mode is shown in Figure 5. The frequencies of all of the simulated HOMs were measured with a greatest deviation of $\sim 0.2\%$ and no missing or extra modes were found.

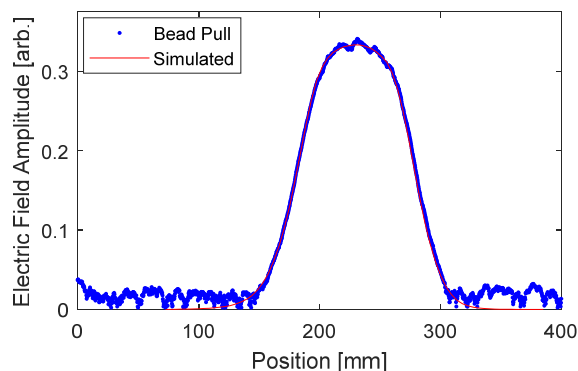


Figure 5: Bead pull measurement of the operating mode showing good agreement to the simulated field profile.

CONCLUSION

The fabrication of the Nb cavity has commenced using bulk reactor grade niobium. The TIG welding procedure has been developed and will be applied for the cavity welds in a glove box with less than 10 ppm oxygen. Fabrication of the copper prototype has validated the fabrication procedures and all measurements made compare well with the RF design.

ACKNOWLEDGMENT

The author's travel to IPAC'17 has been supported by the Division of Physics of the United States National Science Foundation (Accelerator Science Program) and the Division of Beam Physics of the American Physical Society.

REFERENCES

- [1] S.R. Koscielniak *et al.*, in *Proc. IPAC'17*, TUPAB022, 2017.
- [2] S.U. De Silva and J. R. Delayen, *Phys. Rev. ST Accel. Beams*, vol. 16, p. 082001, 2013.
- [3] D.W. Storey *et al.*, in *Proc. SRF'15*, THBP044, 2015.
- [4] C.A. Cooper, A. Wu, P. Bauer, and C. Antoine, *IEEE Trans. Appl. Supercond.*, vol. 19, p. 1399, 2009.
- [5] C. Compton *et al.*, in *Proc. SRF'07*, WEP01, 2007.